CDF note 10064

Updated Measurement of the $B_s^0 \to \phi\phi$ Branching Ratio Using 2.9fb^{-1}

The CDF Collaboration
URL http://www-cdf.fnal.gov
(Dated: February 3, 2010)

We present a study of the $B_s^0 \to \phi\phi$ decay using a sample of $2.9 fb^{-1}$ of Tevatron data collected with the displaced track trigger of the upgraded Collider Detector at Fermilab (CDF II). Signals of $B_s^0 \to \phi\phi$ and $B_s^0 \to J/\psi\phi$ decays are reconstructed and their yields measured. The $B_s^0 \to J/\psi\phi$ is used as a normalization mode in the measurement of the $B_s^0 \to \phi\phi$ branching ratio ($\mathcal{B}$). We measure $R = \mathcal{B}(B_s^0 \to \phi\phi)/\mathcal{B}(B_s^0 \to J/\psi\phi) = [1.78 \pm 0.14(stat) \pm 0.20(syst)] \cdot 10^{-2}$. We then extract the $B_s^0 \to \phi\phi$ Branching Ratio using the world average value of $\mathcal{B}(B_s^0 \to J/\psi\phi)$. The result is: $\mathcal{B}(B_s^0 \to \phi\phi) = [2.40 \pm 0.21(stat) \pm 0.27(syst) \pm 0.82(BR)] \cdot 10^{-5}$, where the last error is due to the uncertainty in the $\mathcal{B}(B_s^0 \to J/\psi\phi)$.

I. INTRODUCTION

Charmless B_s^0 decays currently are copiously produced at the Tevatron and represent a field still to be fully explored that offers additional ways to test our present theoretical understanding. The $B_s^0 \to \phi\phi$ belongs to a particular class of these decays: the B_s^0 meson decays into a CP eigenstate final state consisting of a pair of vector mesons ($B_s^0 \to VV$). It can thus be used to measure the B_s^0 decay width difference ($\Delta\Gamma_s$) and CP violation in the interference between decay and mixing. Moreover the rich dynamics of the $B_s^0 \to VV$ decay, involving three different amplitudes for the three different polarizations of the decay products, makes this channel attractive to test the detailed theoretical predictions for these polarization amplitudes.

The $B_s^0 \to \phi\phi$ decay proceeds through a $b \to s\bar{s}s$ quark level process, and, in the Standard Model (SM), the dominant diagram is the $b \to s$ penguin. The same penguin amplitude is involved in several processes which have shown some discrepancies with the SM predictions raising considerable attention on the theoretical side. Solutions invoking both new physics or SM effects have been put forward to explain the experimental data. To shed light on this rather complex scenario, new and more precise measurements are clearly needed in as many interesting channels as possible. The study of $B_s^0 \to \phi\phi$ channel is an important element of this experimental effort.

The $B_s^0 \to \phi\phi$ decay has been observed for the first time by CDF II in 2005 [1] in a data sample corresponding to 180 pb^{-1} of integrated luminosity; 8 events have been counted and a first measurement of its CP averaged Branching Ratio has been performed obtaining $\mathcal{B}(B_s^0 \to \phi\phi)) = [1.4 \pm 0.6(stat) \pm 0.6(syst)] \cdot 10^{-5}$. Notice that here and in the following charge conjugate decay modes are implied unless otherwise stated. In this note we present an updated measurement with an integrated luminosity of $2.9 fb^{-1}$ of $p\bar{p}$ collision data collected with the displaced track trigger of the upgraded Collider Detector at Fermilab (CDF II).

We reconstruct the $B_s^0 \to J/\psi\phi$ decay in the same dataset, and use this decay as a normalization mode. The $B_s^0 \to J/\psi\phi$ is topologically similar and allows the extraction of the $B_s^0 \to \phi\phi$ Branching Ratio without any uncertainty due to the B_s to B_d production cross section ratio.

The measurement described here represents the first step in a more detailed analysis of $B_s^0 \to \phi\phi$ decays including polarization currently under way. A preliminary result on a related B^0 decay mode has been presented in ref. [2].

II. DETECTOR TRIGGER AND DATA SAMPLE

The CDF II detector is described in detail elsewhere [3]. Most relevant to this analysis are the tracking and trigger systems. Hadronic B decays are collected via a dedicated track trigger capable of identifying tracks displaced from the primary vertex due to the long lifetime of b-hadrons. The online track reconstruction is performed first in the central drift chamber by the XFT track processor [4] and by the Silicon Vertex Tracker [5] at the second level trigger. The latter combines the drift chamber and silicon vertex informations achieving impact parameter resolution similar to offline.

The analysis described here uses a data sample selected requiring two tracks with transverse momenta $p_T \geq 2GeV/c$ and with 120 $\mu m \leq d_0 \leq 1.0$ mm. Furthermore the two trigger tracks must have an opening angle in the transverse plane satisfying $2^\circ \leq |\Delta\phi| \leq 90^\circ$ and must satisfy the requirement $L_{xy} \geq 200$ μm, where the two dimensional decay length, L_{xy}, is calculated as the transverse distance from the beam line to the two track vertex projected along the total transverse momentum of the track pair. Three slightly different requirements on the scalar sum of track transverse momenta, $p_{T1} + p_{T2}$, define the three subsamples used for this measurement. That is `B_CHARM_LOWPT` requires $p_{T1} + p_{T2} > 4$GeV/c, `B_CHARM` ask for opposite charge tracks and $p_{T1} + p_{T2} > 5.5$GeV/c while `B_CHARM_HIGHPT` ask for opposite charge tracks with $p_{T1} + p_{T2} > 6.5$GeV/c. The three different subsample are combined together after taking in to account the different effective luminosity integrated by each of them due to varying trigger prescale factor applied online in order to keep the total trigger rate manageable.

In the following we will refer to *exclusive trigger configurations*. These are defined as follow:

- `B_CHARM_HIGHPT`: events selected by `B_CHARM_HIGHPT`;
- `B_CHARM && !B_CHARM_HIGHPT`: events selected by `B_CHARM` but not by `B_CHARM_HIGHPT`;
- `B_CHARM_LOWPT && !B_CHARM_HIGHPT && !B_CHARM_HIGHPT`: events selected by `B_CHARM_LOWPT` but neither by `B_CHARM` nor by `B_CHARM_HIGHPT`.

Planar drift chambers [6] are used to identify muons with different transverse momentum thresholds due to geometry and material in front of them. For pseudo-rapidity $\eta \lesssim 0.6$ the CMU and CMP chambers can identify muons with $p_T > 1.5$GeV/c, while for pseudo-rapidity $0.6 <\lesssim \eta \lesssim 1.0$ CMX chambers have a threshold of approximately 2 GeV/c.

The sample has been collected in the data taking period from beginning of RunII till April 2008, and the integrated luminosity (without accounting for prescale factors) is 2.9 ± 0.2fb^{-1}.

We reconstruct the B_s^0 decay to two $\phi(1020)$ vector mesons with $\phi(1020) \to K^+K^-$ (BR=$49.2 \pm 0.6\%$ [7]), the final states thus consists of 4 charged kaons emerging from a single displaced vertex. We reconstruct the $B_s^0 \to J/\psi\phi$ decay using $J/\psi \to \mu^+\mu^-$ and $\phi(1020) \to K^+K^-$ decays leading in a $\mu^+\mu^-K^+K^-$ combination from a single displaced vertex also in this case. To reconstruct B candidates all four-track combinations where at least two of them satisfy trigger criteria are fit to a common vertex. All the tracks used in the vertex fit are required to have both drift chamber and silicon vertex hits and a minimum transverse momentum of 400 MeV/c. Opposite charge track pairs with invariant mass within 15 MeV/c^2 from the PDG [7] $\phi(1020)$ mass are considered $\phi(1020)$ candidates. In the case of the $B_s^0 \to J/\psi\phi$ vertex fit a mass constraint is also employed, imposing that the two muon candidates from J/ψ decay have invariant mass equal to the J/ψ world average mass. This constraint significantly improves the invariant mass resolution of the measured $\mu^+\mu^-K^+K^-$ mass. At least one of the two tracks from the J/ψ decay is required to have a confirmation in the muon detectors located outside of the calorimeters which can detect muons with momentum above 1.5 GeV/c. With this requirement an abundant and clean sample of $B_s^0 \to J/\psi\phi$ events is collected, keeping to a negligible level the contamination from $J/\psi \to e^+e^-$ decays. The selected $B_s^0 \to J/\psi\phi$ sample with just one muon leg identified is an interesting sample per se since it identify a largely independent sample with respect to the one collected with the dedicated J/ψ triggers and used for the most precise $\Delta\Gamma_s$ and β_s measurements to date [8].

III. OPTIMIZATION PROCEDURE

No signal peak is visible after applying offline the trigger cuts and a loose vertex fit quality, as can be seen in Fig. 1. Huge backgrounds due to random track combinations and to $\phi(1020)$ production from heavy flavor decays combined with two other random tracks need to be reduced in order to identify the $B_s^0 \to \phi\phi$ signal. A set of cuts on discriminating variables already introduced in [1] has been optimized in order to minimize the statistical uncertainty in the branching ratio measurement. The standard figure of merit $F = \mathrm{S}/\sqrt{\mathrm{S}+\mathrm{B}}$, where S is the number of expected signal events from Monte Carlo simulation and B is the background taken from the sidebands, has been maximized varying independently the individual cuts in a fairly large range of reasonable values. Monte Carlo events were generated using the latest available versions of the generator packages used in CDF, BGen([9]) for producing single B mesons according to a p_T spectrum derived from data [10] and EvtGen([11]) for decaying unstable particles in the final state.

Background in the peak region of the B_s^0 mass is estimated by defining two sidebands, one from 5.02 to 5.22 GeV/c^2 and the other one from 5.52 to 5.72 GeV/c^2. Signal Monte Carlo events are normalized to data signal events selected as in the previous CDF publication [1], and then used in the optimization procedure after applying the identical selection as in data.

The variables used for signal selection optimization are chosen based on their low correlation, agreement between Monte Carlo and Data distribution, effectiveness in discriminating signal from background. In particular the variables that we optimized in the $B_s^0 \to \phi\phi$ case are the following:

- L_{xy}: transverse decay length of the reconstructed B vertex projected along the B transverse momentum;
- $d0^{B_s}$: impact parameter of the reconstructed B meson momentum with respect to the beam line center;
- χ^2_{xy}: χ^2 of the common vertex fit;
- $d0^{\phi}_{max}$: impact parameter of the more energetic ϕ particle.
- $\mathrm{P}_T^{K\,\mathrm{min}}$: transverse momentum of the least energetic K candidate.

All of the above discriminating variables are shown in Fig. 2-6 for sideband, sideband subtracted signal data events and Monte Carlo signal events. For all of the variables a good agreement between data and Monte Carlo is achieved ensuring that the optimization procedure is unbiased.

For the $B_s^0 \to J/\psi\phi$ mode, after the decay vertex fit, at least one of the two muon tracks from the $J/\psi \to \mu^+\mu^-$ decay is required to match to a muon segment either in the central (pseudo-rapidity $\eta < 0.6$) muon detectors (CMU or CMP) or in the forward (CMX) muon detectors.

A set of further cuts is optimized with a procedure similar to what described above for the $B_s^0 \to \phi\phi$ case. The following discriminating variables are used:

- L_{xy}: transverse decay length of the reconstructed B vertex projected along the B transverse momentum;
- $d0^{B_s}$: impact parameter of the reconstructed B meson momentum direction with respect to the beam line center;
- χ^2_{xy}: χ^2 of the common vertex fit;

- P_T^{ϕ}: transverse momentum of the ϕ candidate;
- $\mathrm{P}_T^{J/\psi}$: transverse momentum of the J/ψ candidate.

The cut values are summarized in the Table I, and Table II

Variable	Cut
L_{xy}	> 330 μm
$\mathrm{P}_T^{K\,\mathrm{min}}$	> 0.7 GeV/c
$d0^{\phi}_{max}$	> 85 μm
χ^2_{xy}	< 17
$d_0{}^B$	< 65 μm

TABLE I: *Optimized cut values for $B_s^0 \to \phi\phi$ selection.*

Variable	Cut
L_{xy}	> 290 μm
P_T^{ϕ}	> 1.36 GeV/c
$\mathrm{P}_T^{J/\psi}$	> 2.0 GeV/c
χ^2_{xy}	< 18
$d_0{}^B$	< 65 μm
confirmation of ≥ 1 muon	

TABLE II: *Optimized cut values for $B_s^0 \to J/\psi\phi$ selection.*

IV. BACKGROUNDS

The expected backgrounds have been evaluated by a combination of Monte Carlo simulations as well as an analysis of reflections from known decay modes using data.

For the normalization mode $B_s^0 \to J/\psi\phi$ the dominant decay that enters as a reflection in the invariant mass window of the signal is the $B^0 \to J/\psi K^{*0}$ decay, where the $K^{*0} \to K^+\pi^-$, when reconstructed as K^+K^-, falls inside the $\phi(1020)$ mass window. The background fraction $f_{J/\psi K^{*0}} = N(B^0 \to J/\psi K^{*0})/N(B_s^0 \to J/\psi\phi)$ of $B^0 \to J/\psi K^{*0}$ peaking under the B_s^0 signal is estimated using:

$$f_{J/\psi K^{*0}} = \frac{f_d}{f_s}\frac{\mathcal{B}(B^0 \to J/\psi K^{*0})}{\mathcal{B}(B_s^0 \to J/\psi\phi)}\frac{\mathcal{B}(K^{*0} \to K^+\pi^-)}{\mathcal{B}(\phi \to K^+K^-)}\frac{\varepsilon^{J/\psi K^{*0}}(J/\psi\phi)}{\varepsilon^{J/\psi\phi}}, \tag{1}$$

where $\varepsilon^{J/\psi K^{*0}}(J/\psi\phi)$ is the trigger and selection efficiency of the $B^0 \to J/\psi K^{*0}$ decay reconstructed as a $B_s^0 \to J/\psi\phi$ one and $\varepsilon^{J/\psi\phi}$ is the trigger and selection efficiency for $B_s^0 \to J/\psi\phi$, both estimated using Monte Carlo simulation. The other parameters are extracted from the PDG [7]; f_d and f_s are the production fractions of the B_d and B_s mesons.

From this formula we obtain $f_{J/\psi K^{*0}} = 0.0419 \pm 0.0093$; the large error is mostly due to the uncertainties in branching ratios and in the $\frac{f_d}{f_s}$ ratio.

For the $B_s^0 \to \phi\phi$ the following decays that could produce reflections in the B_s^0 mass window have been considered:

$$B^0 \to \phi K^{*0} \to K^+K^-K^+\pi^-$$
$$B_s^0 \to \overline{K}^{*0}K^{*0} \to K^-\pi^+K^+\pi^-.$$

The background contributions are calculated using:

$$N(B^0 \to \phi K^*) = \frac{f_d}{f_s}\frac{\mathcal{B}(B^0 \to \phi K^{*0})}{\mathcal{B}(B_s^0 \to J/\psi\phi)}\frac{\mathcal{B}(K^{*0} \to K^+\pi^-)}{\mathcal{B}(J/\psi \to \mu\mu)}\frac{\varepsilon^{\phi K^*}(\phi\phi)}{\varepsilon^{J/\psi\phi}}N(B_s^0 \to J/\psi\phi) \tag{2}$$

$$N(B_s^0 \to \overline{K^{*0}}K^{*0}) = \frac{\mathcal{B}(B_s^0 \to \overline{K^{*0}}K^*)}{\mathcal{B}(B_s^0 \to J/\psi\phi)} \frac{\mathcal{B}(K^{*0} \to K^+\pi^-)}{\mathcal{B}(J/\psi \to \mu\mu)} \frac{\mathcal{B}(K^{*0} \to K^+\pi^-)}{\mathcal{B}(\phi \to K^+K^-)} \frac{\varepsilon^{\overline{K^*}K^*}(\phi\phi)}{\varepsilon^{J/\psi\phi}} \cdot N(B_s^0 \to J/\psi\phi), \quad (3)$$

where $\varepsilon^{\phi K^*}(\phi\phi)$ and $\varepsilon^{\overline{K^*}K^*}(\phi\phi)$ are respectively the $B^0 \to \phi K^*$ and $B_s^0 \to \bar{K^{*0}}K^{*0}$ efficiency to be reconstructed as a $B_s^0 \to \phi\phi$ decay. These efficiencies are evaluated using Monte Carlo generated events. For $B_s^0 \to \overline{K^{*0}}K^{*0})$ decay we use the expected theoretical branching ratio, $\approx 9 \cdot 10^{-6}$, quoted in [13].

reflection	$\varepsilon(\phi\phi)$	number of events
$B_s^0 \to \bar{K^{*0}}K^{*0}$	$\sim 10^{-6}$	0
$B^0 \to \phi K^{*0}$	$(0.0134 \pm 0.0002)\%$	8 ± 3

TABLE III: *Number of events and efficiencies for the $B_s^0 \to \phi\phi$ reflections.*

The efficiency and expected number of background events are reported in Table III. Since the overall efficiency for the $B_s^0 \to \bar{K^{*0}}K^{*0}$ to be reconstructed as a $B_s^0 \to \phi\phi$ is very low, we will neglect its contribution in the following.

We don't expect other B-meson or baryon decays to produce significant peaking background in the vicinity of the B_s^0 mass peak.

V. MEASUREMENT OF THE SIGNAL YIELDS

Applying the optimized cuts the invariant mass distributions, m_{KKKK} for the $B_s^0 \to \phi\phi$ and $m_{J/\psi KK}$ for $B_s^0 \to J/\psi\phi$, are obtained, shown respectively in Fig. 8 and 9.

In these distributions clear peaks from the signals are visible, along with two kinds of background:

- **combinatoric background**: these are random combinations of charged tracks, possibly including real ϕ meson decays, and accidentally satisfying the selection requirements. They produce a smooth mass distribution. It is the more important source of background in our analysis.
- **physics background**: it is due to partially reconstructed heavy flavor decays or to an incorrect mass assignment to the tracks of other B meson decays (reflections). We expect a distribution peaking underneath the signal (as detailed in the previous section).

An empirical parametrization for the latter components as well as for signal using Monte Carlo simulation has been derived, in order to perform a fit on our data sample to extract the signal yields.

The signal is parametrized with two Gaussian functions having the same mean value but different resolutions to account for possible detector effects that may cause an additional spread of the tail of the mass distributions. The ratio between the two widths (3.2) and the fraction of the signal under the narrow width (95%) have been fixed by fit of the Monte Carlo signal mass distributions.

The reflection, simulated with Monte Carlo, can be parametrized with a Gaussian having different widths on the two side of the peak plus a decreasing exponential function. In the fit to data all the parameters determining the shape of the reflections are fixed.

The combinatoric background within the considered mass window and its invariant mass distribution follows, with a good approximation, an exponentially decreasing behavior.

A binned maximum likelihood fit is performed taking into account all the components described above, free parameters are the signal fraction, position of the B_s^0 mass peak and peak width, together with the exponential slope defining the combinatorial background mass shape and total number of events.

In conclusion, we obtain the number of $B_s^0 \to J/\psi\phi$ events in the sample:

$$N_{J/\psi\phi} = frac \cdot n_{TOT} = 1766 \pm 48(\text{stat}) \quad (4)$$

where the statistical uncertainty accounts for the uncertainty on both the signal fraction (the actual fit parameter) and the total number of events (the correlation is always negligible). The position of the mass peak is consistent with the known B_s^0 mass and the narrow Gaussian width is around 9.5 MeV/c^2.

Repeating the same fit using the different trigger subsamples described above, we derive the trigger composition for the available data sample shown in Tab.IV.

Trigger path	fractions
B_CHARM_HIGHPT	0.416 ± 0.021
B_CHARM && !B_CHARM_HIGHPT	0.326 ± 0.018
B_CHARM_LOWPT && !B_CHARM_HIGHPT && !B_CHARM_HIGHPT	0.259 ± 0.016

TABLE IV: *Event fractions of different trigger configurations for* $B_s^0 \to J/\psi\phi$.

The events collected by the displaced track trigger do not completely overlap with the sample of the same decay collected via the dedicated JPSI trigger, mostly due to the lower p_T threshold for muons possible in this analysis. To quantify this overlap, and hence the additional statistics collected by the displaced track trigger, the events which are uniquely collected through the latter have been selected in order to obtain the B_s^0 candidate mass distribution shown in Fig. 10. A simplified fit with a single Gaussian and an exponential combinatorial background shape gives 1100 ± 40 events. This additional sample represents a sample of one third the size of the one used with the same integrated luminosity in the measurement of the B_s^0 mixing phase [8]. Work is in progress in order to include these events in the B_s^0 mixing phase analysis, although it may be anticipated that the effective statistical power of the additional sample may be degraded due to the inherent bias in the lifetime distribution introduced by the displaced track trigger.

A similar analysis has been performed for the $B_s^0 \to \phi\phi$ candidates. Signal and reflection parametrization are derived from Monte Carlo following the same functional forms used for the $B_s^0 \to J/\psi\phi$ case. The number of $B_s^0 \to \phi\phi$ events is then determined as:

$$N_{\phi\phi} = 295 \pm 20(\text{stat}) \tag{5}$$

where the uncertainty takes into account the full correlation matrix of the fit results.

In Table V we summarize the fractions of events for different trigger configurations, using the same fit on sample selected using the exclusive trigger combinations discussed above.

Trigger path	fractions
B_CHARM_HIGHPT	0.394 ± 0.048
B_CHARM && !B_CHARM_HIGHPT	0.377 ± 0.048
B_CHARM_LOWPT && !B_CHARM_HIGHPT && !B_CHARM_HIGHPT	0.223 ± 0.037

TABLE V: *Fractions for the different trigger configurations for the* $B_s^0 \to \phi\phi$ *decay.*

VI. MEASUREMENT OF $B_s^0 \to \phi\phi$ BRANCHING RATIO

The branching ratio $\mathcal{B}$ of the decay $B_s^0 \to \phi\phi$, normalized to the known $\mathcal{B}B_s^0 \to J/\psi\phi$, can be evaluated using the following formula:

$$\frac{\mathcal{B}(B_s^0 \to \ \phi\phi)}{\mathcal{B}(B_s^0 \to J/\psi\ \phi)} = \frac{N_{\phi\phi}}{N_{J/\psi\phi}} \cdot \frac{\mathcal{B}(J/\psi \to \mu\mu)}{\mathcal{B}(\phi \to K^+K^-)} \cdot \frac{\varepsilon_{TOT}^{J/\psi\phi}}{\varepsilon_{TOT}^{\phi\phi}} \cdot \varepsilon_{\mu}^{TOT} \tag{6}$$

where $N_{J/\psi\phi}$ and $N_{\phi\phi}$ are respectively the number of $B_s^0 \to J/\psi\phi$ events and the number of $B_s^0 \to \phi\phi$ events in our sample; $\varepsilon_{TOT}^{J/\psi\phi}$ and $\varepsilon_{TOT}^{\phi\phi}$ are the combined trigger and selection efficiencies derived from MC simulation. The term ε_{μ}^{TOT} accounts for the efficiency of the requirement of identifying at least one of the muons in the muon detectors.

Using the ratio of Eq.6 the uncertainties in the cross section of B meson production cancel out as well as several systematic effects due to the detector and trigger efficiencies, allowing a reduced systematic uncertainty in the measurement of the BR.

A. Trigger and Selection Efficiencies

The efficiencies for both $B_s^0 \to \phi\phi$ and $B_s^0 \to J/\psi\phi$ channels are obtained computing the ratio between the number of events that satisfy the various trigger and selection criteria (with the same set of cuts used for the signal selection in the data) and the number of generated events.

The trigger and selection efficiencies are estimated separately for different exclusive trigger configurations (see Tables VII and VI). In the same Tables the second column report the efficiency when the Monte Carlo B_s^0 p_T spectrum is re-weighted to match the observed p_T spectrum in data. The latter will be our default value for the present measurement.

exclusive trigger configuration	ε_i (%)	p_T re-weight (%)
B_CHARM_HIGHPT	0.3500 ± 0.0042	0.3650 ± 0.0043
B_CHARM && !B_CHARM_HIGHPT	0.2533 ± 0.0036	0.2411 ± 0.0035
B_CHARM_LOWPT && !B_CHARM_HIGHPT && !B_CHARM_HIGHPT	0.4238 ± 0.0046	0.3986 ± 0.0045
Sum	1.0271 ± 0.0071	

TABLE VI: *Trigger and selection efficiencies of the $B_s^0 \to J/\psi\phi$ for exclusive trigger configurations, with and without the p_T re-weight procedure.*

exclusive trigger configuration	ε_i(%)	p_T re-weight (%)
B_CHARM_HIGHPT	0.3631 ± 0.0013	0.3713 ± 0.0014
B_CHARM && !B_CHARM_HIGHPT	0.2654 ± 0.0011	0.2686 ± 0.0012
B_CHARM_LOWPT && !B_CHARM_HIGHPT && !B_CHARM_HIGHPT	0.4729 ± 0.0015	0.4310 ± 0.0015
Sum	1.1014 ± 0.0024	

TABLE VII: *Trigger and selection efficiencies of the $B_s^0 \to \phi\phi$ for exclusive trigger configurations, with and without the p_T re-weight procedure.*

Thus, the total efficiency is given by:

$$\varepsilon_{TOT} = \sum_i p_i \varepsilon_i \tag{7}$$

where p_i and ε_i are, respectively, the prescale factor (related to the different dataset an the particular trigger configuration) and the efficiency of each exclusive trigger (in our case: B_CHARM_HIGHPT, B_CHARM && !B_CHARM_HIGHPT and B_CHARM_LOWPT && !B_CHARM_HIGHPT && !B_CHARM_HIGHPT). The final value for the efficiency ratio is:

$$\frac{\varepsilon_{rec}^{J/\psi\phi}}{\varepsilon_{TOT}^{\phi\phi}} = 0.939 \pm 0.030 \pm 0.009 \tag{8}$$

The first uncertainty includes the uncertainty coming from limited Monte Carlo statistics (negligible) and the dominant uncertainty from the observed fractions of $B_s^0 \to J/\psi\phi$ data candidates in the three different trigger paths. The second uncertainty comes from the variation within errors of the re-weighting function parameters. The latter largely cancel in the efficiency ratio thus ensuring a limited impact on the final uncertainty from the limited knowledge of the B_s^0 meson p_T spectrum.

Ignoring trigger prescaling would cause the efficiency ratio to be just 0.8% lower than the quoted value implying a relatively minor impact of the uncertainty due to trigger prescaling on the measurement, which is well covered by the assigned systematics.

B. Muon Efficiency

The efficiency for the muon identification requirements is derived, in a data-driven way, separately from the trigger and reconstruction efficiencies discussed above. The simulation do not properly account for the muon acceptance and the related uncertainty would not cancel in the ratio of efficiency because this request is only applied to the $B_s^0 \to J/\psi\phi$ sample.

The requirement on the muons for the channel $B_s^0 \to J/\psi\phi$ is that the J/ψ candidates have at least one of the two tracks with a match in the muon detectors. The efficiency for muon identification has been determined as a function of

muon p_T in two different pseudo-rapidity regions corresponding to the CMU/CMP and CMX detectors. In a second step, this function is used to calculate the efficiency for selecting at least one muon out of two using the p_T muon spectra provided by the Monte Carlo simulation of the $B_s^0 \to J/\psi\phi$ decay before applying the muon identification criteria.

We evaluate the efficiency on an inclusive sample of $J/\psi \to \mu\mu$ collected through the same trigger as our data sample. In doing so, we are sure that the data has been collected under the same exact trigger prescale and instantaneous luminosity conditions as in our signal data samples.

The J/ψ signal peak region (60 MeV/c^2 wide) is defined as $M_{\mu,\mu} \in [3.072, 3.132]\text{GeV}/c^2$, corresponding approximately to a $\pm 2\sigma$ region. The efficiency for muon identification has been determined, after sideband subtraction, calculating the fraction of J/ψ candidates with two muons identified over the number of J/ψ candidates with 1 or 2 muons identified in the muon chambers.

We parametrize the efficiency as a function of p_T obtained for both the CMU and CMX regions (see Fig. 11) with a sigmoid function whose parameters are determined by a χ^2 fit using Minuit:

$$\varepsilon(p_T) = \frac{A}{1 + e^{[B(p_T + C)]}} \tag{9}$$

The measured efficiencies with overlaid the fit function are reported in Fig. 11 for CMU and CMX regions. The parameter values for the efficiency function obtained from a binned χ^2 fit are reported in Table VIII.

	A	B	C
CMU	0.8404± 0.0057	1.76 ± 0.19	-1.435 ± 0.084
CMX	0.6815± 0.0077	2.88 ± 0.25	-2.084 ± 0.026

TABLE VIII: *Parameter values of the sigmoid functions used to fit the muon efficiency distributions of Fig.11.*

Using the muon efficiency as a function of p_T and the p_T spectrum of muons from simulated $B_s^0 \to J/\psi\phi$ decays after trigger and kinematics selection, we calculate the average efficiency in our sample for finding at least one of the J/ψ muon legs with a matching stub in the muon detectors.

Assuming the efficiency for the first and second muon to be uncorrelated we obtain the per event efficiency for reconstructing at least 1 muon among the two J/ψ decay tracks using the following formula:

$$\varepsilon_{\mu,\,i}^{TOT} = \varepsilon(p_{T1})_i \cdot [1 - \varepsilon(p_{T2})_i] + \varepsilon(p_{T2})_i \cdot [1 - \varepsilon(p_{T1})_i] + \varepsilon(p_{T1})_i \cdot \varepsilon(p_{T2})_i \tag{10}$$

where $(p_{T1,2})_i$ are the transverse momenta of the two muon tracks (1,2) from the i-th J/ψ candidate decay, and the efficiencies are the CMU or CMX ones according to the muon pseudo-rapidity. The average of the per event efficiency over all the J/ψ candidates in the $B_s^0 \to J/\psi\phi$ Monte Carlo sample, will give the needed efficiency.

Including the statistical uncertainty from the turn-on parameter fit errors (from Table VIII) and their correlation we finally obtain:

$$\varepsilon_{\mu}^{TOT} = 0.8695 \pm 0.0044(\text{stat}).$$

VII. SYSTEMATIC UNCERTAINTIES

Several systematic effects has been considered originating from both our limited knowledge of the physics parameters (like Branching Ratios and polarization in the decay) and from uncertainties in the measurement itself or data modeling.

The most relevant effects studied here are:

- uncertainties on the number of events obtained in Sec.V and due to:
  - the variation in the fit mass range in order to account for the possible presence of unidentified peaking background near the signal peak and uncertainty in the combinatorial background shape;
  - the parametrization of the signal with only one Gaussian functions instead of two as in the default signal model.
- uncertainties on the background subtraction, coming mostly from uncertainty in the Branching Ratio used in the calculation of the background;

- uncertainty on the muon efficiency discussed in section VI B;
- uncertainty on the ratio of the trigger and selection efficiencies due to the following effects:
  - the polarization of $B_s^0 \to J/\psi\phi$ and $B_s^0 \to \phi\phi$ decays and the related average lifetime differences between the two decay channels. The $B_s^0 \to \phi\phi$ polarization has been varied between completely longitudinal to completely transverse keeping transverse parallel and tranverse perpendicular proportion equal. The $B_s^0 \to J/\psi\phi$ polarization has been varied within the world average uncertainties. Finally, the width difference ratio $\Delta\Gamma_s/\Gamma_s$ has been varied in the range $0.06 < \Delta\Gamma_s/\Gamma_s < 0.18$;
  - uncertainty in the the p_T spectrum re-weight from the comparison of Monte Carlo and $B_s^0 \to J/\psi\phi$ data;
  - the effect due to the different particles types involved in the final states ($\mu\mu KK$ and $KKKK$) related to the particle dependence of the XFT efficiency [12].
- uncertainty due to the Branching Ratio of the normalization channel.

	$B_s^0 \to \phi\phi$	$B_s^0 \to J/\psi\phi$
	$\Delta N_{\phi\phi}/N_{\phi\phi}$	$\Delta N_{J/\psi\phi}/N_{J/\psi\phi}$
fit range	3%	-
signal parametrization	3%	2%
background subtraction: error on BRs	1%	1%
	$\Delta\varepsilon_{\phi\phi}/\varepsilon_{\phi\phi}$	$\Delta\varepsilon_{J/\psi\phi}/\varepsilon_{J/\psi\phi}$
polarization in MC	7%	6%
	$\Delta\varepsilon_{\phi\phi}/\varepsilon_{J/\psi\phi}$	
XFT particle dep.	4%	
p_T re-weight	0.9%	
	$\Delta\varepsilon_{\mu}/\varepsilon_{\mu}$	
η parametrization & correlation	0.9%	

TABLE IX: *Summery of fractional systematic uncertainties in the measurement of* $\mathcal{B}(B_s^0 \to \phi\phi)$.

In Table IX we summarize the systematic uncertainties for the measurement of the BR. Summing in quadrature the various contribution we derive a total relative systematic uncertainty of 11% not considering the $B_s^0 \to J/\psi\phi$ Branching Ratio error.

VIII. RESULTS

We studied the $B_s^0 \to \phi\phi$ and $B_s^0 \to J/\psi\phi$ decays using a sample of $2.9 fb^{-1}$ collected using the displaced track trigger in CDF II since 2002 until April 2008.

The number of events obtained for two decays channels are:

$$\begin{aligned} N_{\phi\phi} &= 295 \pm 20(\text{stat}) \pm 12(\text{syst}) \\ N_{J/\psi\phi} &= 1766 \pm 48(\text{stat}) \pm 41(\text{syst}) \end{aligned}$$

Using the formula of Eq.6, we obtain:

$$\frac{\mathcal{B}(B_s^0 \to \phi\phi)}{\mathcal{B}(B_s^0 \to J/\psi\phi)} = [1.78 \pm 0.14(stat) \pm 0.20(syst)] \cdot 10^{-2}$$

.

We can then use the Branching Ratio of $B_s^0 \to J/\psi\phi$ from PDG[7], updated to reflect the more recent measurements of the ratio of production cross section of B_s and B_d mesons [15] to derive:

$$\mathcal{B}(B_s^0 \to \phi\phi) = [2.40 \pm 0.21(stat) \pm 0.27(syst) \pm 0.82(BR)] \cdot 10^{-5}$$

The last uncertainty (BR) is the dominant contribution and arises only from the error of the BR ($B_s^0 \to J/\psi\phi$).

	$\mathcal{B}(B_s^0 \to \phi\phi) \cdot 10^5$
QCDF(1) [13]	$2.18 \pm 0.11\ ^{+3.04}_{-1.70}$
QCDF(2) [13]	$1.95 \pm 0.10\ ^{+1.31}_{-0.80}$
pCDF [14]	$3.53\ ^{+0.83}_{-0.69}\ ^{+1.67}_{-1.02}$

TABLE X: *Theoretical predictions for $BR(B_s^0 \to \phi\phi)$ from two recent papers.QCDF(2) differs from QCDF(1) because certain amplitudes have been constrained from a fit to other existing $B \to VV$ experimental data.*

Comparing this result with that of the first publication [1], we see that there is a good agreement and a substantial improvement on the statistical uncertainty. Recent theoretical calculation of this Branching Ratio are reported in both QCDF [13] and pQCD [14] (Table X) in both cases with large uncertainty of order $\pm 1 \cdot 10^{-5}$. The present result is consistent with both theoretical calculations within uncertainties even if at the low end pf the allowed range from [14].

In addition we have isolated an independent sample of $B_s^0 \to J/\psi\phi$ decays from that collected with the dedicated `DI_MUON` trigger, which is normally used in CDFII to study such decays (Fig. 10). The yield measured in this channel with the dataset collected with the the displaced track trigger corresponds to a 30 % increase in the CDF sample size of $B_s^0 \to J/\psi\phi$ decays with the same integrated luminosity as used here.

Acknowledgments

We thank the Fermilab staff and the technical staffs of the participating institutions for their vital contributions. This work was supported by the U.S. Department of Energy and National Science Foundation; the Italian Istituto Nazionale di Fisica Nucleare; the Ministry of Education, Culture, Sports, Science and Technology of Japan; the Natural Sciences and Engineering Research Council of Canada; the National Science Council of the Republic of China; the Swiss National Science Foundation; the A.P. Sloan Foundation; the Bundesministerium für Bildung und Forschung, Germany; the World Class University Program, the National Research Foundation of Korea; the Science and Technology Facilities Council and the Royal Society, UK; the Institut National de Physique Nucleaire et Physique des Particules/CNRS; the Russian Foundation for Basic Research; the Ministerio de Ciencia e Innovación, and Programa Consolider-Ingenio 2010, Spain; the Slovak R&D Agency; and the Academy of Finland.

[1] D.Acosta et al. (CDF Collaboration),*Phys. Rev. Lett.* **95**, 031801, 2005.
[2] CDF coll., *Measurement of the polarization amplitudes in $B \longrightarrow J/\psi K^*$ and $B \longrightarrow \phi K^*$ using Two Track Trigger at CDF*, CDF Note n 8096, July 2006, available at: http://www-cdf.fnal.gov/cdfnotes/cdf8096_BdtoVV_v1.0.ps
[3] The CDF II Detector Technical Design Report, Fermilab-Pub-96/390-E; D. Acosta, et al., Phys. Rev. D **71**, 032001 (2005).
[4] E.J. Thomson, et al., IEEE Trans. on Nucl. Science., **49**, 1063 (2002).
[5] W. Ashmanskas, et al., Nucl. Instrum. Methods A **518**, 532 (2004).
[6] G. Ascoli et al., Nucl. Instrum. Methods, A **268**, 33 (1988).
[7] Particle Data Group; Phys. Lett. **B667**, 1 (2008).
[8] CDF Public Note 9458, available at: http://www-cdf.fnal.gov/physics/new/bottom/080724.blessed-tagged_BsJPsiPhi_update_prelim/public_note.pdf
[9] K. Anikeev, C. Paus, P. Murat, *Description of Bgenerator II*, CDF Note n.5092, August 1999.
[10] Mary Bishai,*et al.Measurement of the b-Hadron Inclusive Cross-section in CDF Run II using $b \to J/\psi\ X$* CDF Note n.6285
[11] D. Lange, A. Ryd, *The EvtGen Event Generator Package*, CHEP proceedings 1998.
[12] CDF coll.,*CP Asymmetries and Decay Rate Ratios of Cabibbo suppressed D^0 Decays* CDF Note n 6391, August 2004, available at: http://www-cdf.fnal.gov/physics/new/bottom/031211.blessed-d0/blessed-d0.ps .
[13] M. Beneke, J. Rohrer and D. Yang, Nucl. Phys. B **774**, 64 (2007) [arXiv:hep-ph/0612290].
[14] A. Ali, G. Kramer, Y. Li, C. D. Lu, Y. L. Shen, W. Wang and Y. M. Wang, Phys. Rev. D **76**, 074018 (2007) [arXiv:hep-ph/0703162].
[15] The PDG value for $\mathcal{B}(B_s^0 \to J/\psi\phi) = (0.93 \pm 0.33) \cdot 10^{-3}$ is based on a single CDF Run I measurement that assumed $f_s/f_d = 0.40$. We scale the central value to reflect the current (PDG 2008 [7]) value of $f_s/f_d = 0.110/0.399 = 0.28$. Hence we use:$\mathcal{B}(B_s^0 \to J/\psi\phi) = (1.35 \pm 0.46) \cdot 10^{-3}$

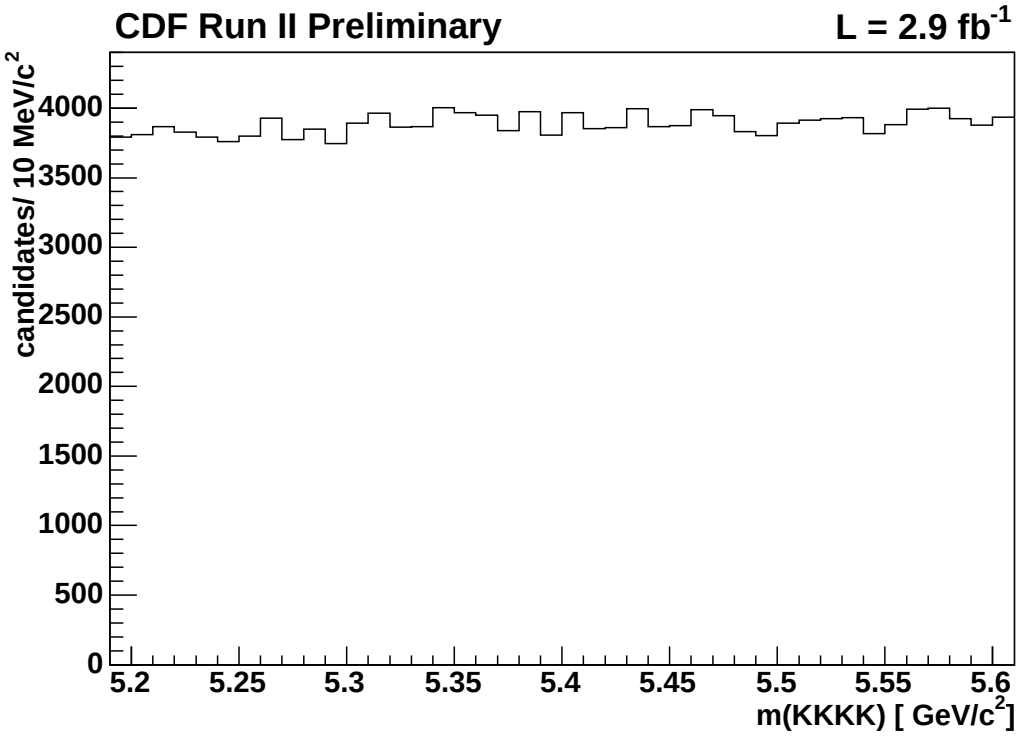

FIG. 1: *KKKK invariant mass after reconstruction and trigger confirmation only.*

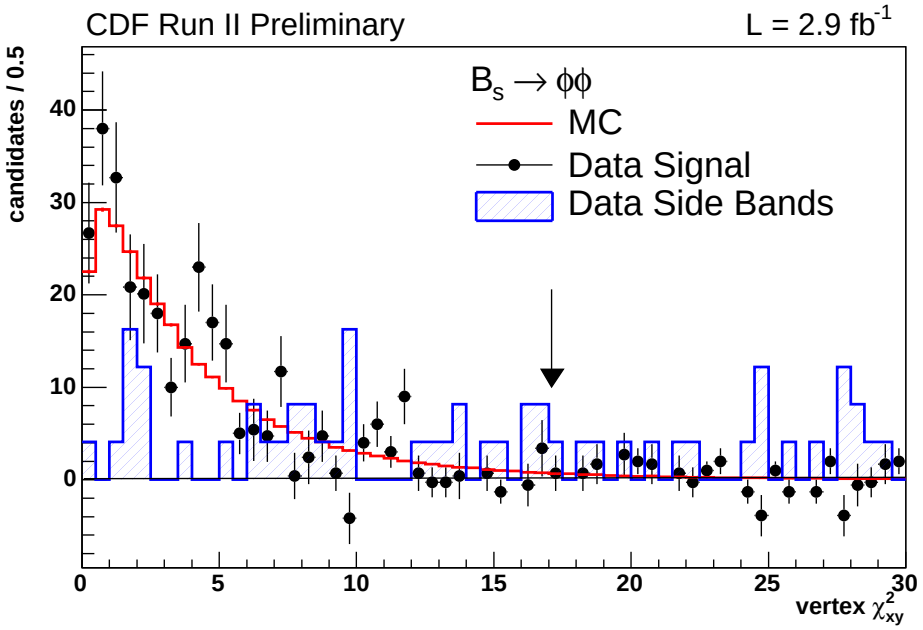

FIG. 2: *Fit vertex χ^2 in the plane transverse to the beam, for sideband subtracted signal, Monte Carlo simulation and B_s^0 mass sidebands. The position of the optimized cut is shown by the arrow.*

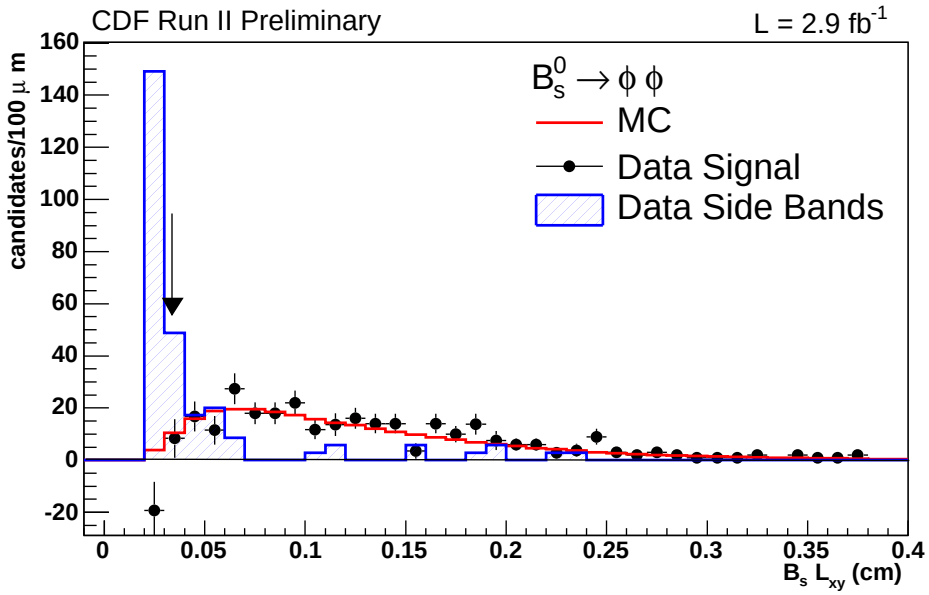

FIG. 3: *Transverse decay length of B_s^0 candidates, for sideband subtracted signal, Monte Carlo simulation and B_s^0 mass sidebands. The position of the optimized cut is shown by the arrow.*

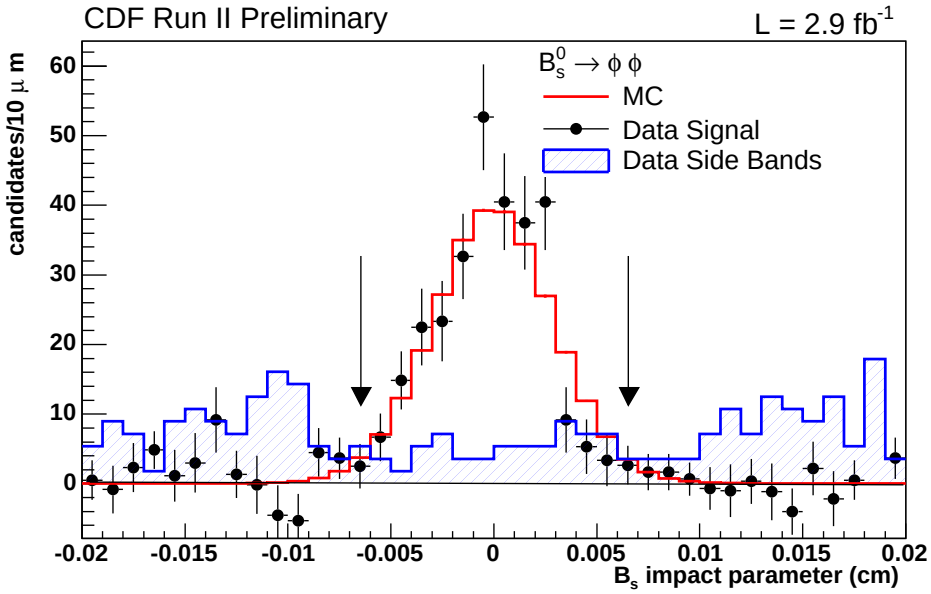

FIG. 4: *Reconstructed impact parameter with respect to the primary vertex of B_s^0 candidates, for sideband subtracted signal, Monte Carlo simulation and B_s^0 mass sidebands. The position of the optimized cut is shown by the arrow.*

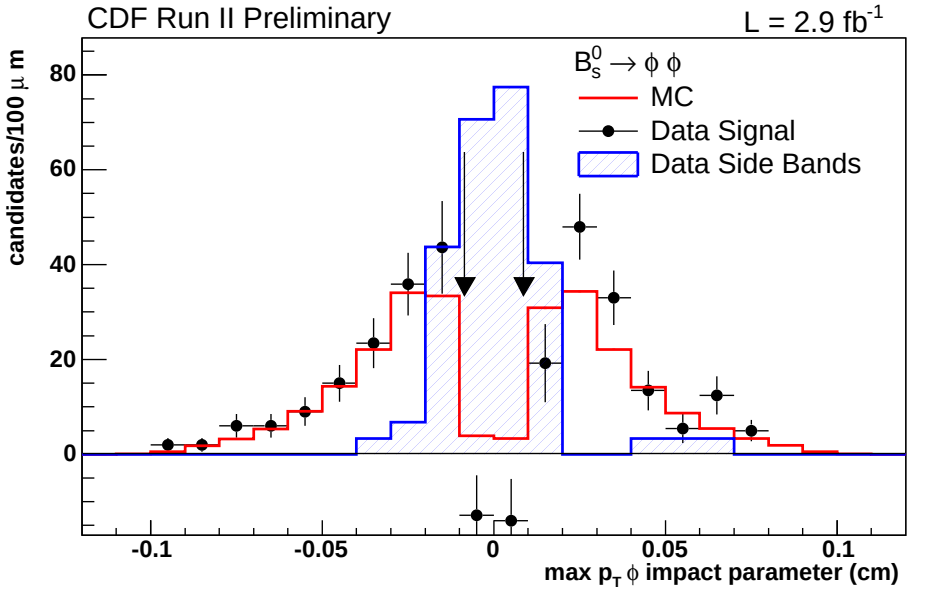

FIG. 5: *Reconstructed impact parameter for the highest momentum phi daughters of $B_s^0 \to \phi\phi$ candidates, for sideband subtracted signal, Monte Carlo simulation and B_s^0 mass sidebands. The position of the optimized cut is shown by the arrow.*

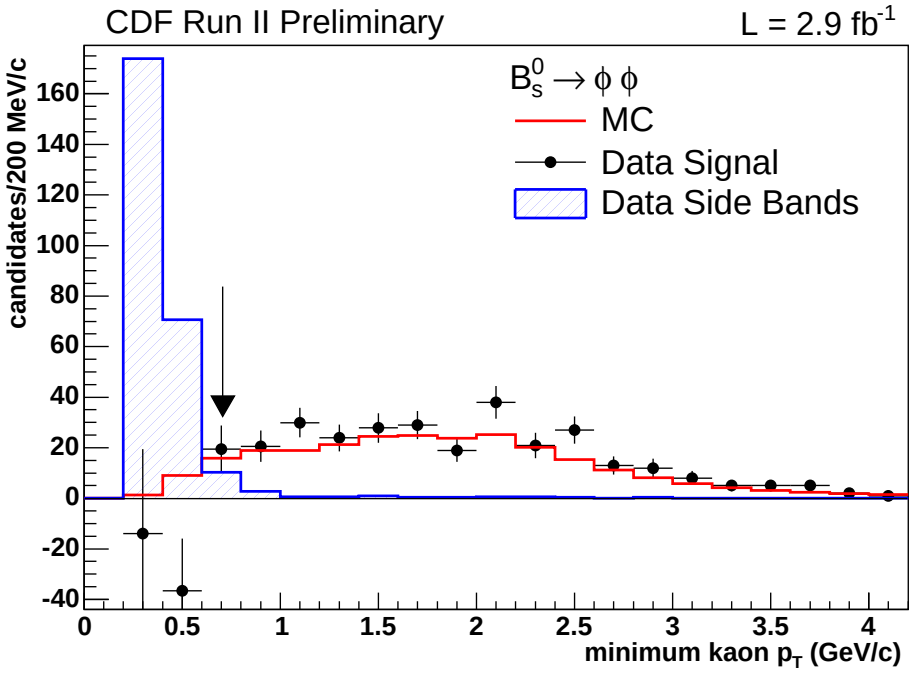

FIG. 6: *Minimum transverse momentum among the 4 kaons in the B_s^0 candidates decays, for sideband subtracted signal, Monte Carlo simulation and B_s^0 mass sidebands. The position of the optimized cut is shown by the arrow.*

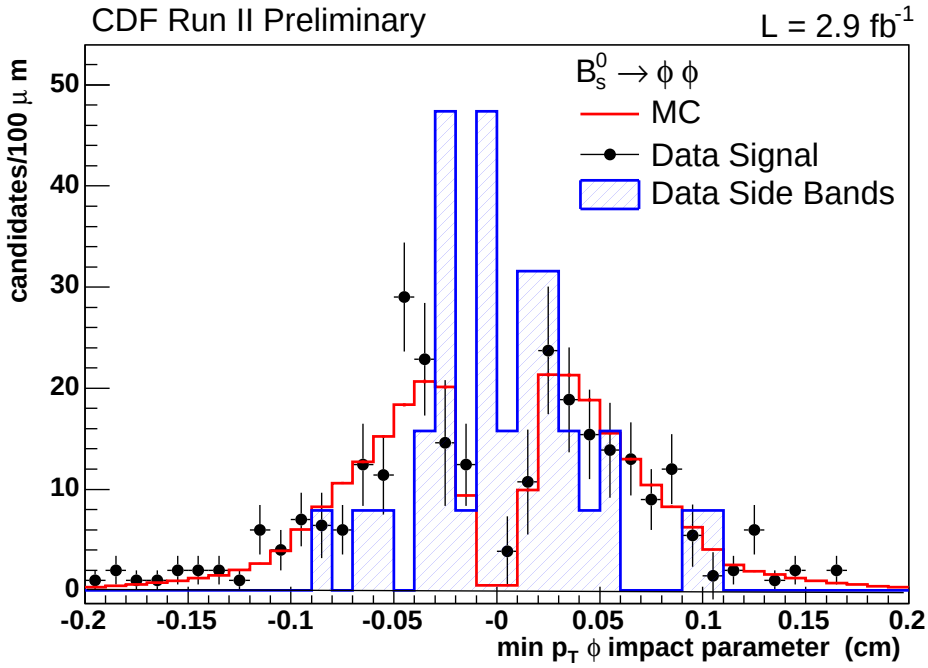

FIG. 7: *Reconstructed impact parameter for the lowest momentum phi daughters of $B_s^0 \to \phi\phi$ candidates, for sideband subtracted signal, Monte Carlo simulation and B_s^0 mass sidebands. This variable is not used in the actual selection.*

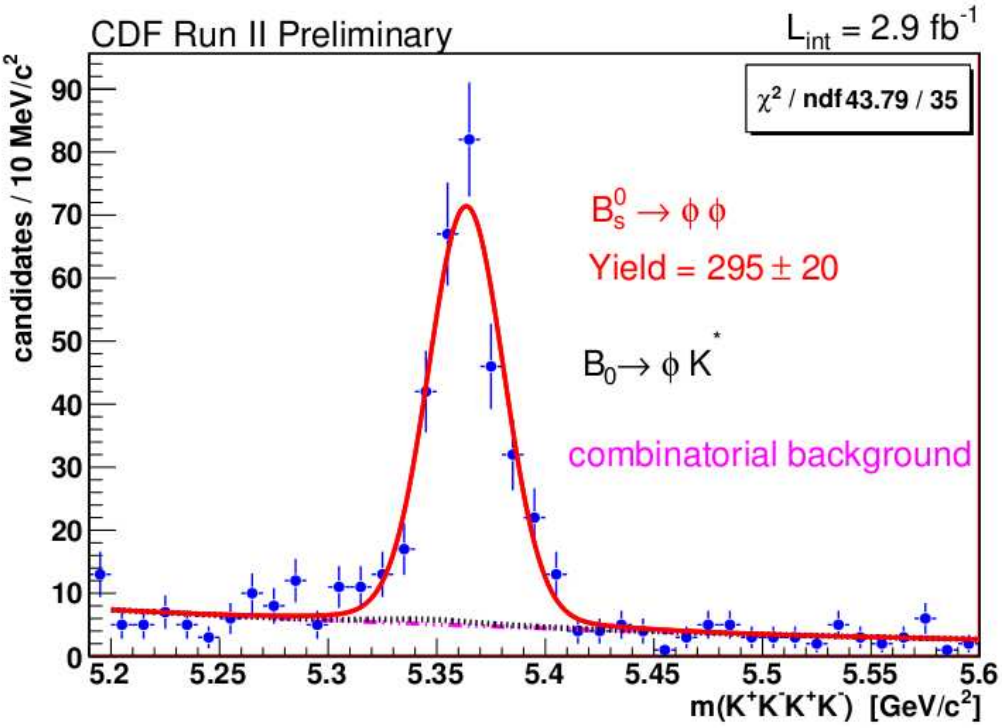

FIG. 8: *KKKK invariant mass with overlaid the fit described in section V to determine the number of* $B_s^0 \to \phi\phi$ *candidates*

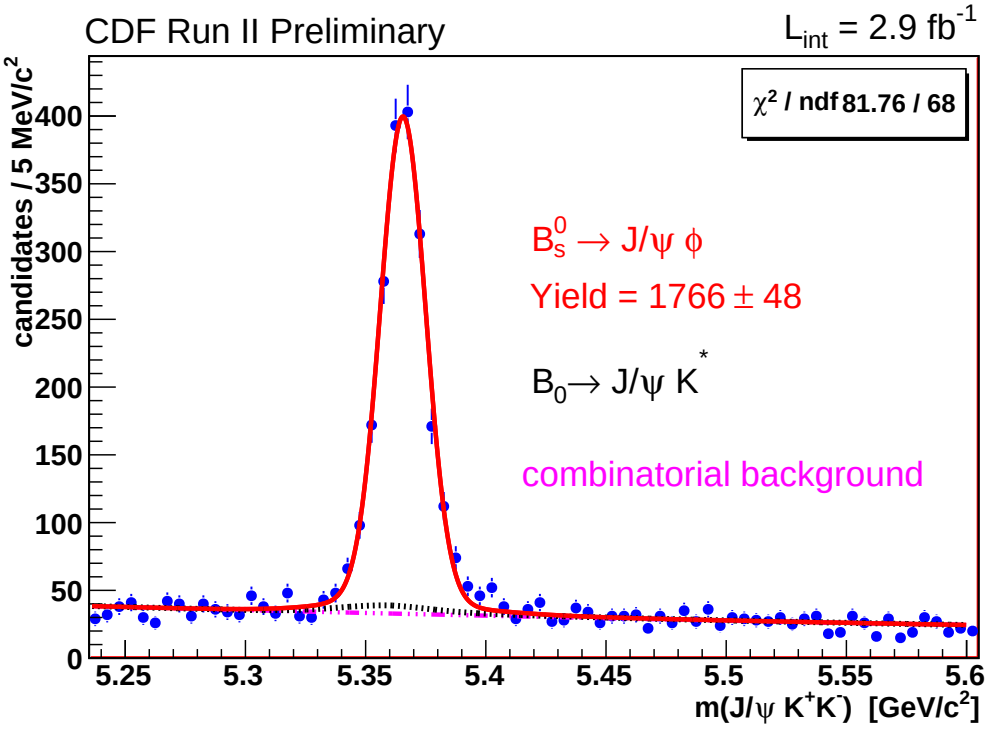

FIG. 9: $J/\psi K^+K^-$ *invariant mass with overlaid the fit described in section V to determine the number of* $B_s^0 \to J/\psi\phi$ *candidates*

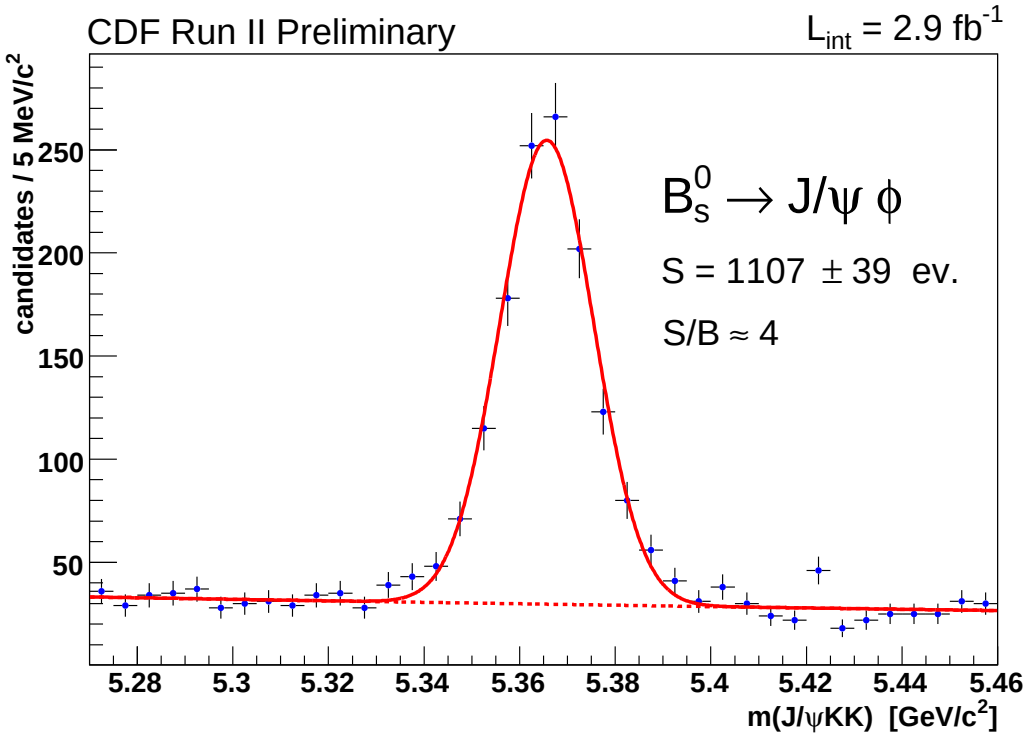

FIG. 10: *$J/\psi K^+K^-$ invariant mass for $B_s^0 \rightarrow J/\psi\phi$ candidates that are exclusively triggered by the displaced track trigger, with overlaid a fit consisting in a signal gaussian on top of an exponential background.*

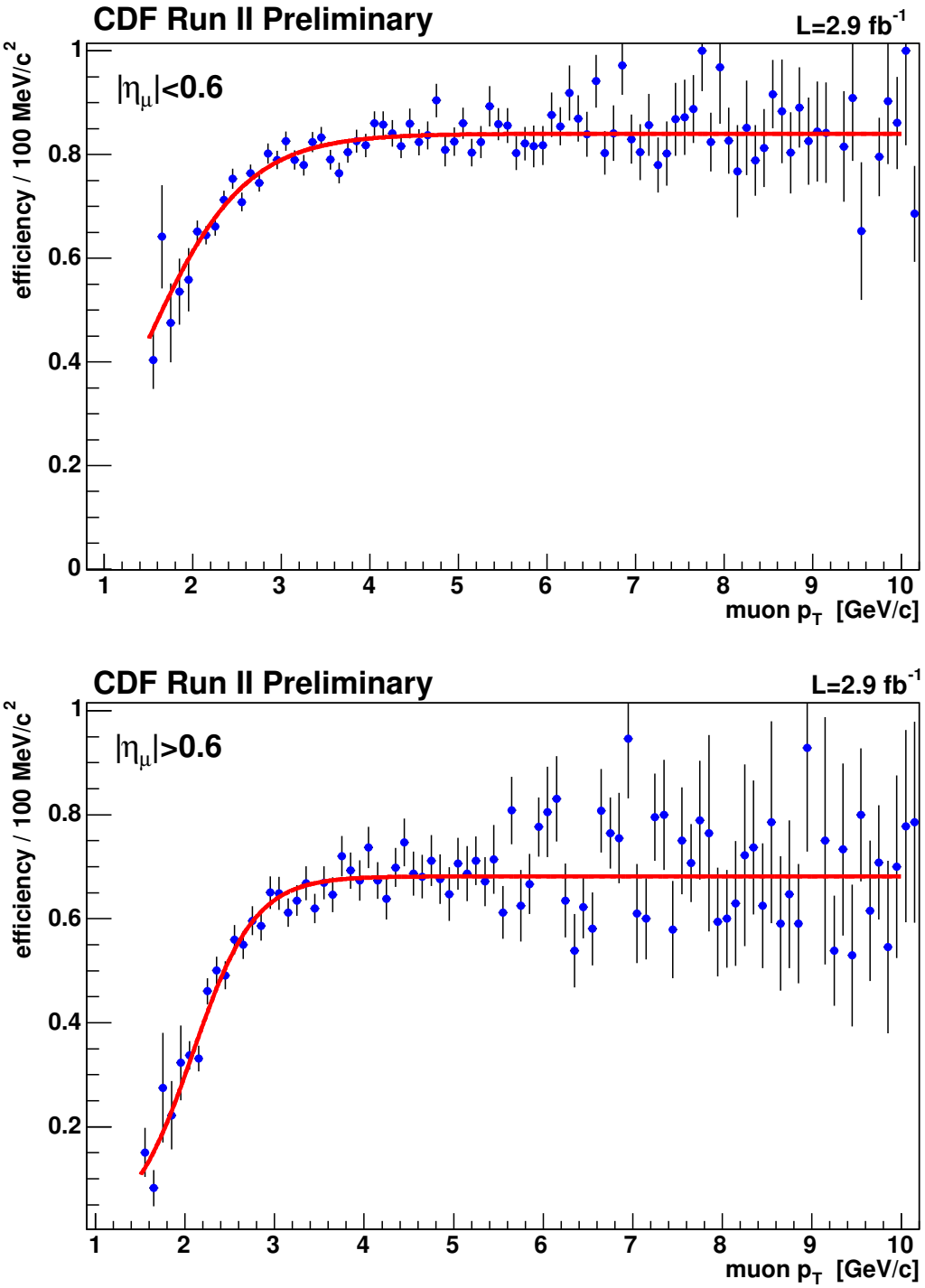

FIG. 11: *Efficiencies as a function of muon transverse momentum: distribution for CMU (up) and CMX (down) muons. All these distributions are fitted with a sigmoid function.*

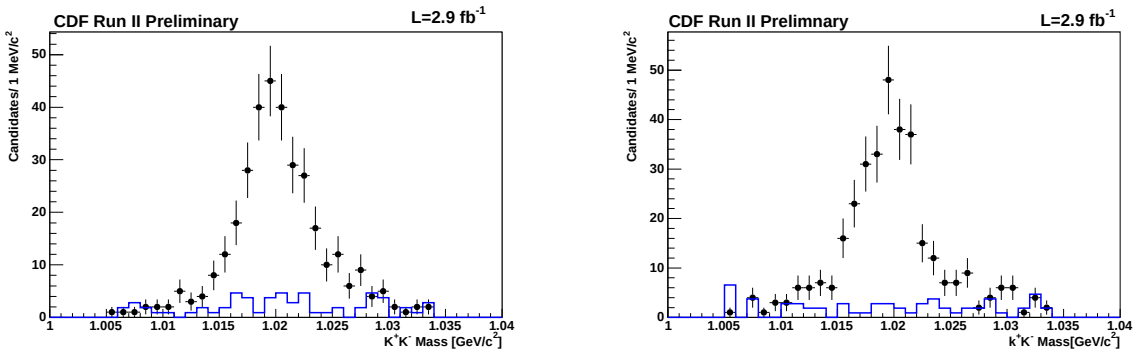

FIG. 12: *Invariant mass for the highest momentum (left) and lower momentum (right) K^+K^- pairs for $B_s^0 \to \phi\phi$ candidates. Points: signal region; blue histogram: B_s^0 mass sideband region.*

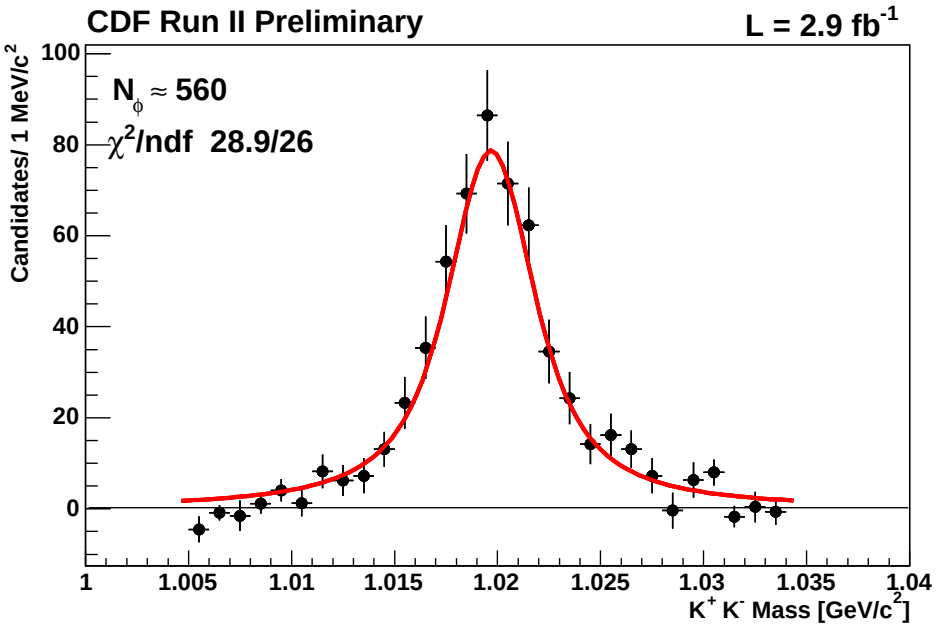

FIG. 13: *Sideband subtracted K^+K^- pair masses (two entries per B_s^0 candidate). The fit (described in text) represents a Breit-Wigner distribution convoluted with a gaussian mass resolution function. In the fit the natural width for the phi meson is fixed to the world average value.*